

ORIGINAL ARTICLE

Investigation of structural and electronic properties of small Au_nCu_m (n+m≤5) nano-clusters for oxygen adsorption

Razieh Habibpour^{1*}; Raheleh Vaziri²

¹Department of Chemical Technologies, Iranian Research Organization for Science and Technology, Tehran, Iran

²Department of Chemistry, Payame Noor University, Tehran, Iran

Received 25 December 2015;

revised 24 April 2016;

accepted 20 May 2016;

available online 01 July 2016

Abstract

In this study, the structures, the IR spectroscopy, and the electronic properties of Au_nCu_m (n+m≤5) bimetallic clusters were studied and compared with those of pure gold and copper clusters using the generalized gradient approximation (GGA) and exchange correlation density functional theory (DFT). The study of an O₂-Au_nCu_m system is important to identify the promotion effects of each of the two metals and their effect in catalysts, sensors, energy sources, or many other applications. This study also demonstrated that the O₂ molecule preferred to adsorb at the Cu site rather than at the Au site in bimetallic clusters. O₂ adsorption at a bridge site is energetically more favored over the other sites (1- both oxygen atoms are bonded to the same substrate atom 2- O₂ is connected to a Cu atom through a single bond) for oxygen adsorption on these clusters. Further, it was concluded that after the adsorption of the O₂ molecule on the bimetallic clusters, the Au-Cu interaction is strengthened and the O-O interaction is weakened; the reactivity improvement of the oxygen molecule was clear.

Keywords: Bimetallic clusters; Density functional theory; Density of states; O₂ adsorption; Vibrational frequency.

How to cite this article

Habibpour R, Raheleh V. Investigation of structural and electronic properties of small Au_nCu_m (n+m≤5) nano-clusters for oxygen adsorption. *Int. J. Nano Dimens.*, 2016; 7(3): 208-217. DOI: [10.7508/ijnd.2016.03.004](https://doi.org/10.7508/ijnd.2016.03.004)

INTRODUCTION

Metal clusters are molecular-like substances designed by assembling a small number of atoms ranging from a few to several hundred. Metal clusters are generally used in nanotechnologies as well as in catalysis. Clusters are distinguished from "bulk" by their specific properties, which depend on the size and composition of the system. These modifications are mainly linked to quantum size effects and to a surface/volume ratio larger than that observed in the solid state [1,2]. One of the foremost reasons for the interest in small clusters is the fact that their chemical and physical properties may be attuned by changing the composition and atomic ordering as well as

the size of the clusters. Their surface structures, compositions, and segregation properties are of interest due to their importance in specifying chemical reactivity. Likewise, bimetallic clusters have attracted attention as they may present structural, electronic, and magnetic properties which are different from those of the pure elemental clusters [3,4]. There are similar cases of pairs of elements (such as Fe and Ag) which are immiscible in the bulk phase but that willingly mix in finite clusters [5].

"Noble metals" such as copper, silver, and gold occur naturally as free metals, but they always contain trace amounts of other noble metals combined into their lattices. Their similar

* Corresponding Author Email: Habibpour@irost.ir

electronegativity and $d^{10}s^1$ electronic structures simplify the alloying of these elements in the solid state. Recently, there has been a growing interest in bimetallic Au/Cu clusters both experimentally and theoretically [6-10]. Although many of the studies emphasized on the structural and electronic properties of the bare bimetallic Au/Cu clusters, still little is known concerning how the mixing of Au and Cu will affect the chemical reactivity of metal clusters into atoms or small molecules. In this report, the interaction between molecular oxygen and small Au_nCu_m ($n + m \leq 5$) clusters is investigated by means of the density functional theory (DFT) [11]. Additionally, the geometry, binding energy, vibrational frequency, density of states, and HOMO-LUMO energies for bimetallic and monometallic clusters were considered.

EXPERIMENTAL

Transition metal clusters have a large number of electrons. In this report, the bimetallic gold-copper clusters were computed using the DFT. DFT methods, which attempt to contain electron correlation effects, have been widely described to be an applied and effective computational tool for metallic clusters. The B3LYP [12] exchange-correlation hybrid functional was selected and appears to give reliable results for the considered systems [5]. Since full electron computation is more time consuming, it is appropriate to present effective core potentials while taking into account some relativistic effects for the Au and Cu atoms in order to describe the inner core electrons. For this reason, the Lanl2DZ [13] basis set was chosen as it deals clearly with valence electrons through a split valence polarized basis set, retaining 19 electrons per Cu atom ($3s^23p^63d^{10}4s^1$) and 19 electrons per Au atom ($5s^25p^65d^{10}6s^1$). The validity of this basis set for copper-gold clusters was recently tested by Yang and coworkers [14] using the same

hybrid exchange–correlation functional (B3LYP). For O_2 molecules, the 6-311G (d,f) basis set was modified, holding 6 electrons per O atom ($2s^22p^4$). The calculation results showed suitable agreement with the available experimental data [15]. All computations and geometry optimizations were carried out using the Gaussian 03 package [16].

All compositions (n/m) were taken into account for the considered nuclearity ($n + m$). The choice of the initial geometry was important to obtain the lowest energy structures. In this study, we gained the most stable structures by considering previous studies regarding the configurations of bare Au/Cu clusters [17,18]; then, we restudied the structural properties of the neutral Au_nCu_m ($n+m \leq 5$) clusters before studying the interaction of Au/Cu clusters with O_2 . All these initial structures were completely optimized by relaxing the atomic positions by minimizing the total energy until the force acting on each atom became negligible. In Table 1, the calculated spectroscopic parameters of the smallest Au_2 , AuCu, and Cu_2 clusters were compared with former experimental data [15,19-21]. The results showed suitable agreement with the experimental values.

RESULTS AND DISCUSSION

Bare Bimetallic Au_nCu_m ($n+m \leq 5$) Clusters




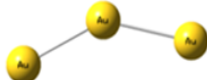

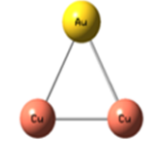
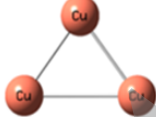


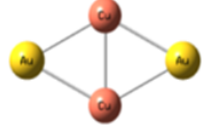
Initially, the structures, the electronic and spectroscopic properties of bare bimetallic Au_nCu_m ($n+m \leq 5$) clusters were studied for comparison with the results of cluster- O_2 complexes. In order to discuss the effects of doped impurity on gold clusters, the required calculations were performed on the pure gold clusters, pure copper clusters, and bimetallic Au_nCu_m clusters. Table 2 displays the results for the most stable monometallic and bimetallic clusters. All the ground states of the Au_nCu_m ($n+m \leq 5$) clusters had a planar structure, and no 3D systems were gained.

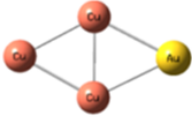

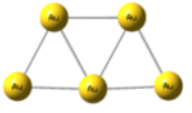
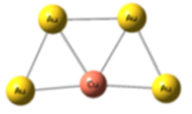
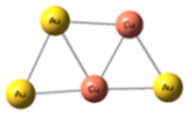
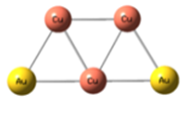
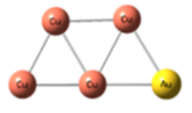
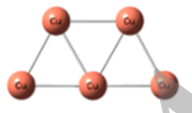
Table 1: Comparison of calculated and experimental values of the bond length (R), Ionization Potential (IP) and vibrational frequencies (Frec.) of Au_2 , AuCu and Cu_2 clusters.

Clusters	Au_2		AuCu		Cu_2	
	Cal.	Exp.	Cal.	Exp.	Cal.	Exp.
R (Å)	2.57	2.47 ^a	2.40	2.33 ^b	2.25	2.22 ^a
IP (ev)	7.18	9.20 ^c	6.39	8.74 ^b	5.59	7.90 ^d
Frec.	162.50	191 ^a	229.12	248 ^b	256.02	265 ^a

^a From Ref. [19], ^b From Ref. [15], ^c From Ref. [20], ^d From Ref. [21].

Table 2: Optimized structure, symmetry, spin multiplicity, dipole moment, average nearest neighbor distance, binding energy, total energy, vibrational frequency, and IR intensity of Au_nCu_m clusters.

	Symmetry	Spin multiplicity	Dipole moment (Debye)	Average nearest neighbor distance (Å)	Binding energy (eV)	Total energy (Hartree)	vibrational frequency (Cm ⁻¹)	IR intensity (Km/mol)
	(D _{∞h})	1	0	2.57	0.93	-270.95	162.5	0
	(C _{∞h})	1	2.63	2.40	1.14	-331.64	229.1	1.874
	(D _{∞h})	1	0	2.25	1.00	-392.31	256.0	0
	(C _{2v})	2	0.37	2.64	0.92	-406.42	150.4	0.008
	(C _{2v})	2	2.49	Au-Au: 2.92 Au-Cu: 2.49	1.15	-467.12	212.4 146.4	5.242 3.030
	(C _{2v})	2	2.11	Cu-Cu: 2.32 Au-Cu: 2.59	1.16	-527.80	234.0 140.5	1.128 1.295
	(C _{2v})	2	0.42	2.48	1.00	-588.46	169.7	8.667
	(D _{2h})	1	0.007	2.74	1.16	-541.93	136.8 62.7	7.550 2.301
	(C _{2v})	1	0.83	Au-Au: 2.73 Au-Cu: 2.57	1.41	-602.64	174.2 66.6	9.265 2.143
	(D _{2h})	1	0.59	Cu-Cu: 2.40 Au-Cu: 2.55	1.61	-663.35	214.2 104.0	20.06 6.800

	(C _{2v})	1	2.04	Cu-Cu: 2.39	1.47	-724.01	215.7	9.891	
				Au-Cu: 2.57			107.7	3.923	
	(D _{2h})	1	0.32	2.42	1.30	-784.66	216.1	7.992	
							109.3	3.634	
<hr/>									
	(C _{2v})	2	1.37	2.76	1.28	-677.43	162.6	3.318	
	(C _{2v})	2	0.62	Au-Au: 2.73 Au-Cu: 2.61	1.45	-738.14	223.7	4.265	
	(C _s)	2	1.31	Au-Au: 2.76 Cu-Cu: 2.50 Au-Cu: 2.56	1.56	-798.84	236.1	11.11	
							192.6	2.383	
	(C _{2v})	2	2.15	Cu-Cu: 2.48 Au-Cu: 2.53	1.58	-859.52	242.6	9.662	
	(C _s)	2	2.74	Cu-Cu: 2.44 Au-Cu: 2.54	1.50	-920.18	191.0	1.493	
							245.9	4.298	
	(C _{2v})	2	0.03	2.43	1.41	-980.84	246.3	1.459	

The triangular structure was the most stable for the triatomic Au_nCu_m (n+m=3) clusters where Au-Cu-Au and Cu-Au-Cu angles were 71.6 and 53.3, respectively. In the case of tetra atomic Au_nCu_m (n+m=4) clusters, the rhombic structure was the most likely structure. The trapezoidal structure with triangular sub-units was the lowest energy structure for the penta atomic (n+m=5) clusters. The most stable structures of the bare clusters we obtained here were in good agreement with the other published literatures [22-25]. The Au-Cu dimer bond distance of 2.40 Å was higher than the Cu-Cu (2.25 Å) bond distance and shorter than the

Au-Au (2.57 Å) bond distance, as shown in Table 2. This was convenient for the charge transfer from Cu to Au. The calculated bond distances were in good agreement with previous theoretical reports [20, 21]. The averaged binding energies of the diatomic systems Au₂ and AuCu were found to be 0.93 and 1.14 eV, respectively, indicating that the Au-Cu bond was stronger than the Au-Au bond. In general, the association of the Cu atom with the most stable bare Au clusters produced the lowest-energy complexes. This study showed that the Cu atom with a smaller atomic radius (R_{Cu}=1.57Å) preferred to exhibit at the center while the Au

atom with a larger size ($R_{Au}=1.79\text{\AA}$) preferred to sit at the edge of the ground state AuCu bimetallic clusters.

The average nearest-neighbor distance was calculated by using the following expression:

$$\bar{R} = 1/n_b \sum_{i,j,i \neq j} R_{ij} \quad (1)$$

Where, R_{ij} is the distance between two atoms i and j with a cutoff = 3.2\AA (which is 15% larger than the corresponding distance in the bulk) and n_b is the total number of bonds between atoms that lie below this cutoff. The nearest neighbor distance in bulk Au is 2.88\AA . The average nearest-neighbor distances in the Au_nCu_m bimetallic clusters are shorter than those in the corresponding monometallic gold clusters, which is due to the different radii between copper and gold atoms. Note that in the bimetallic clusters that have only one Cu atom, the average nearest-neighbor interatomic distances commonly increase with the cluster size. All the ground states of the monometallic Au clusters have an average nearest-neighbor distance of about $2.57\text{--}2.76\text{\AA}$, clearly smaller than the bulk interatomic distance.

The relative stabilities of the clusters are significant parameters for finding the most stable structures. The binding energy (E_b) equation can be defined as:

$$E_b = [nE(Au) + mE(Cu) - E(Au_nCu_m)] / (n + m) \quad (2)$$

The calculated E_b for the stable clusters are shown in Table 2 in which the average E_b slowly increases with the increase in the cluster size. The bimetallic Au_nCu_m clusters with approximately the same number of atoms of Au and Cu had the highest E_b .

The stability of the cluster depends on its E_b and vibrational intensity. The infrared spectra of monometallic and bimetallic clusters will be studied and discussed in detail in this section. For each cluster structure, the stability is determined by calculating the frequency of the harmonic vibration. The harmonic vibrational frequencies of the clusters were also calculated to reveal the dynamical stability and bond stiffness of the systems. It is generally observed that (Table 2) the Au based clusters have lower vibrational frequency than the Cu based clusters, which is obviously related to the higher atomic mass of gold. Cu doping in the diatomic gold cluster (AuCu) decreases the average bond length of the

system because of the smaller atomic radius of Cu compared with Au. This decrease is predictable and is accompanied by a bond hardening effect, which is usually visible in the calculated harmonic vibrational frequency of the doped Au cluster. In triatomic clusters with one Cu doping (Au_2Cu), the extent of the reduction in the average bond length and the increase in the vibrational frequency are more than the two Cu doping ($AuCu_2$). In contrast to the bond shortening and hardening effects in the one Cu doping system, we observe that the two Cu doping system has more E_b . It appears that the two doped Cu atoms in the Au cluster inserts an effective amount of electrons in the neighboring bonds, and therefore expiate the observed bond softening. In tetra atomic clusters, it is observed that the bond length decreases in the $Au_4\text{--}Au_3Cu\text{--}Au_2Cu_2\text{--}AuCu_3$ series while the absolute binding energy and vibrational frequency increases. Subsequently, the Au-Cu bond in the bimetallic clusters has greater strength and stiffness compared with the Au-Au bond in the monometallic Au_4 cluster. The strongest Au-Cu bond is observed in the Au_2Cu_2 cluster with the same number of Au and Cu atoms. A similar trend is seen in the penta atomic clusters. In these systems, the strongest Au-Cu bond was seen in the Au_2Cu_3 cluster. As a consequence of these bond shortening and hardening effects, the Cu doping raises the absolute binding energy of the Au clusters.

The dipole moment in a cluster is an important property. It is generally used to study the intermolecular interactions because the higher the dipole moment, the intermolecular interactions are stronger. There is a correlation between the dipole moment, binding energy, and stability of the cluster. The dipole moment of the clusters obtained using DFT calculation are provided in Table 2. The calculated dipole moment for the bimetallic Au_nCu_m clusters with the less Cu atom is higher than other bimetallic and monometallic clusters.

Fig. 1 shows the electronic density of states (DOS) for the Au_nCu_m clusters. The electronic properties of the Au_nCu_m clusters are discussed by examining the HOMO (highest occupied molecular orbital) and LUMO (lowest unoccupied molecular orbital) and the energy gap between them. The HOMO-LUMO gap (HLG) is a useful measure for examining the stability of clusters. It is observed that systems with greater HLG's are, in general, less

reactive. In other words, the gap reflects the ability of electrons to jump from the occupied orbital to the unoccupied orbital; it also represents the ability for the molecular participates to produce chemical reactions to some degree. The HOMO–LUMO orbital pictures of the Au_nCu_m clusters are given in Fig. 1. The positive and negative phases are represented in red and green colors, respectively. A generally valid linear correlation relationship exists between the calculated HOMO energies and the experimental/calculated ionization potentials; between the calculated LUMO

energies and experimental/calculated electron affinities; between the calculated average HOMO/LUMO energies and electronegativity values; and between the calculated HOMO-LUMO energy gaps and hardness/softness values. Consequently, the calculated HOMO and LUMO energies can be used to semi-quantitatively estimate the ionization potentials (IPs), electron affinities (EAs), electronegativity (χ), global hardness (η), and softness (σ) [26]. These quantum chemical parameters were measured using Equations (3)-(5) and their values were listed in Table 3.

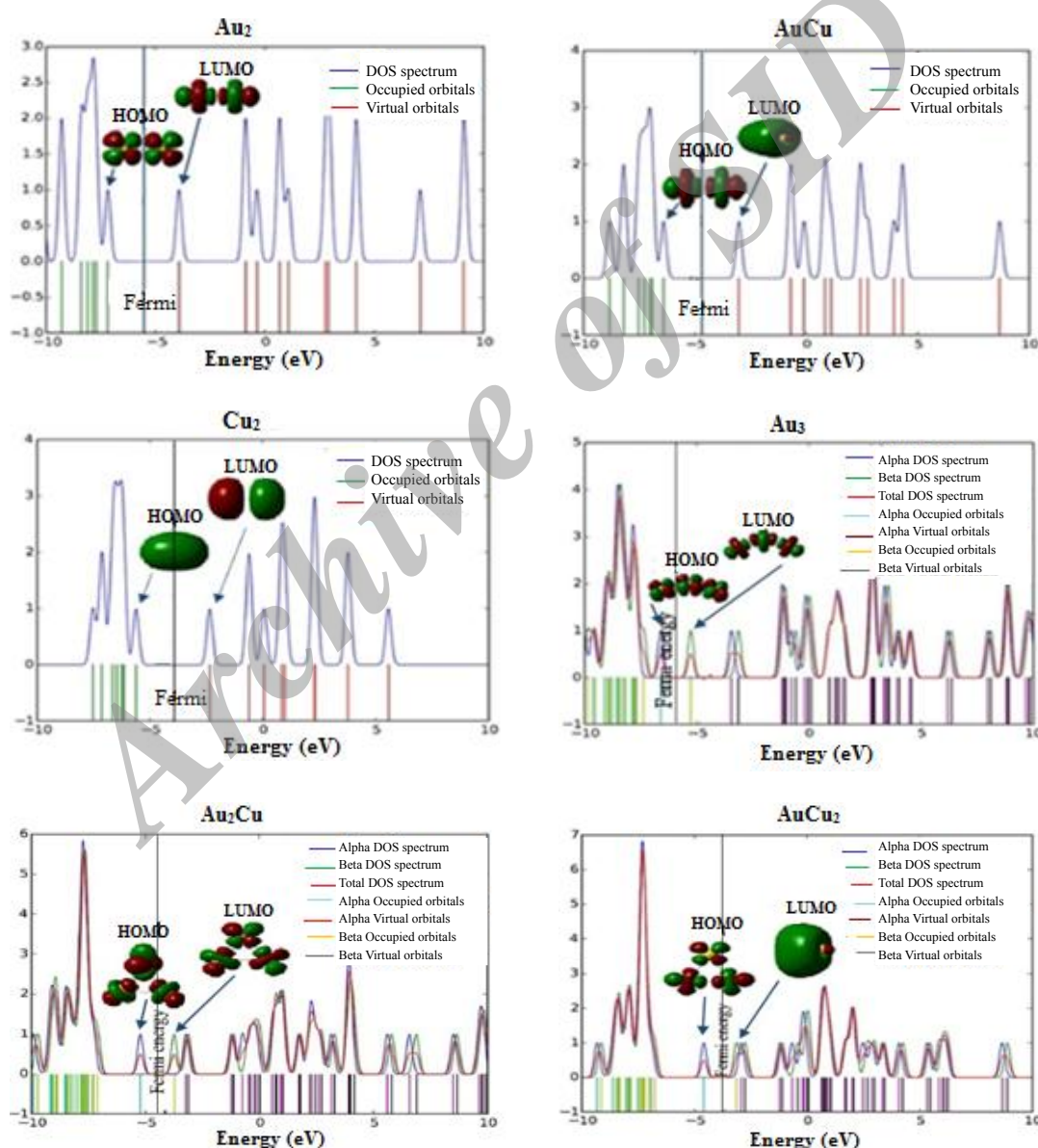


Fig. 1: Density of states, spatial orientation of HOMO and LUMO, and Fermi energy of Au_nCu_m clusters. The Fermi energy is the average of the HOMO and LUMO energies.

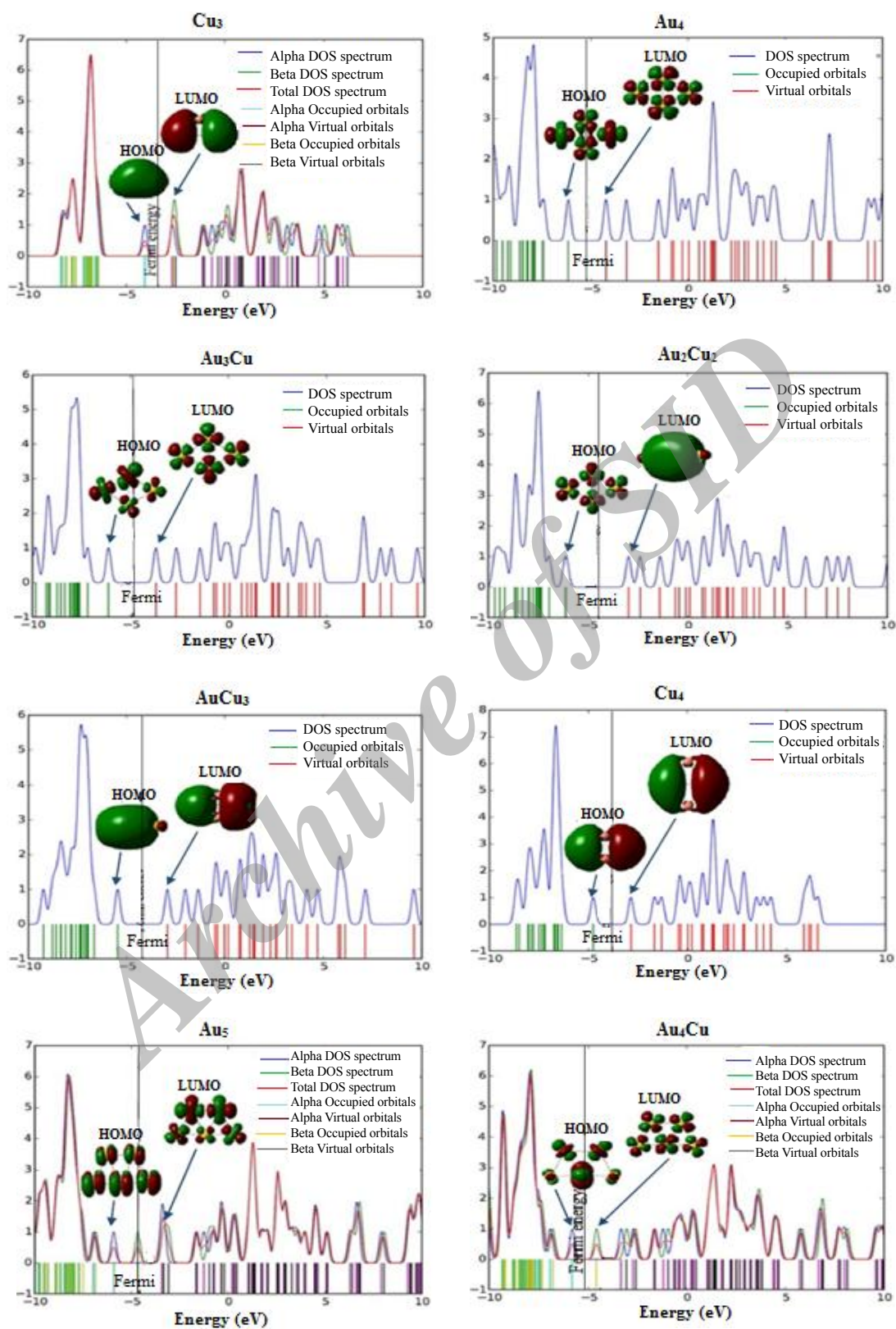


Fig. 1: (Continued) Density of states, spatial orientation of HOMO and LUMO, and Fermi energy of Au_nCu_m clusters. The Fermi energy is the average of the HOMO and LUMO energies.

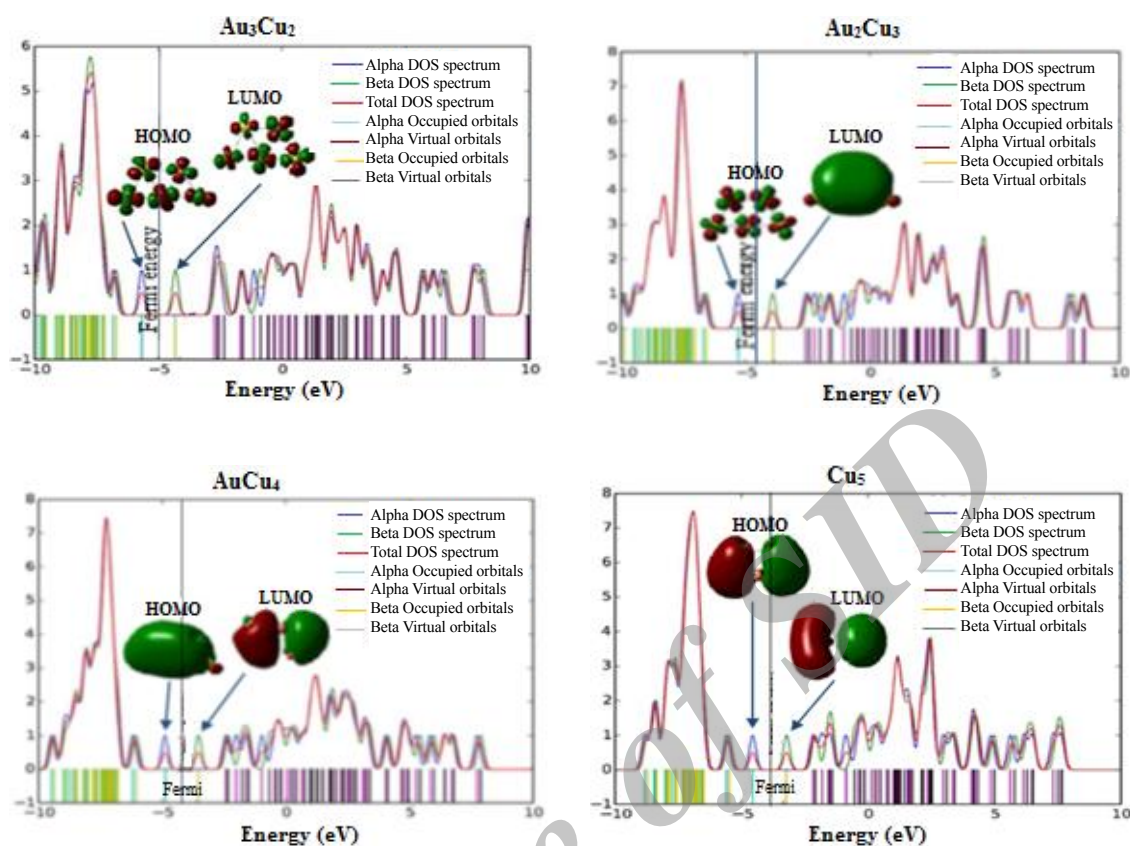


Fig. 1: (Continued) Density of states, spatial orientation of HOMO and LUMO, and Fermi energy of Au_nCu_m clusters. The Fermi energy is the average of the HOMO and LUMO energies.

Table 3: HOMO-LUMO energy gap, Ionization potential, Electron affinity, Electronegativity hardness, and Softness of Au_nCu_m clusters.

	$\Delta E_{\text{HOMO-LUMO}}$	IP	EA	χ	η	σ
Au ₂	3.251	7.1865	3.9320	5.5592	1.6245	0.6155
AuCu	3.376	6.3946	3.0150	4.7048	1.6871	0.5927
Cu ₂	3.254	5.5892	2.3347	3.9619	1.6272	0.6145
Au ₃	1.336	6.5960	2.2572	5.9266	0.6666	1.5001
Au ₂ Cu	1.477	5.2164	3.7361	4.4762	0.7374	1.3561
AuCu ₂	1.450	4.5769	3.1265	3.8504	0.7238	1.3815
Cu ₃	1.393	4.0517	2.6558	3.3551	0.6966	1.4355
Au ₄	1.934	6.1660	4.2286	5.1973	0.9660	1.0351
Au ₃ Cu	2.413	6.1116	3.6953	4.9034	1.2054	0.8296
Au ₂ Cu ₂	3.134	6.1062	2.9769	4.5415	1.5646	0.6391
Au ₃ Cu	2.525	5.4449	2.9197	4.1823	1.2626	0.7920
Cu ₄	1.904	4.7538	2.8364	3.7987	0.9523	1.0500
Au ₅	1.243	5.9075	4.6640	5.2871	0.6204	1.6118
Au ₄ Cu	1.224	5.8014	4.5742	5.1864	0.6122	1.6334
Au ₃ Cu ₂	1.355	5.6518	4.2966	4.9742	0.6775	1.4760
Au ₂ Cu ₃	1.387	5.2871	3.8993	4.5932	0.6938	1.4413
AuCu ₄	1.357	4.8790	3.5211	4.2014	0.6775	1.4760
Cu ₅	1.338	4.5524	3.2136	3.8830	0.6694	1.4938

$$IP = -E_{\text{HOMO}} \quad EA = -E_{\text{LUMO}} \quad (3)$$

Assuming that these relations are valid within the DFT frame, the electronegativity (χ) and hardness (η) can be estimated with:

$$\chi = \left(\frac{IP+EA}{2}\right) \quad \eta = \left(\frac{IP-EA}{2}\right) \quad (4)$$

Softness is given by

$$\sigma = 1/\eta \quad (5)$$

According to Table 3, one can note that the clusters with an even number of atoms have a greater HLG, and therefore are expected to be less reactive than clusters with an odd number of atoms. The stability displayed by the even-number electron clusters is due to their closed-shell configuration that always produces additional stability. The cluster AuCu has the largest HLG of 3.376 eV; therefore, it is the most stable cluster and it has the lowest reactivity. It is usually observed that Cu doping increases the stability of Au clusters. In the triatomic clusters, Au₂Cu has the largest amount of HLG that is in agreement with its larger vibrational frequency and smaller bond length in comparison with Au₃, AuCu₂, and Cu₃. In tetra atomic clusters, Au₂Cu₂ with high symmetry has the largest amount of HLG and the maximum stability in comparison with other tetra atomic clusters.

This result is in agreement with the results of the calculated amount of bond length and vibrational frequency. In penta atomic clusters, Au₂Cu₃ has the largest amount of HLG; therefore, it has the maximum stability which is in agreement with the results and conclusions of the calculated average bond length and vibrational frequency. The χ and σ were applied in several previous works [18,27] to evaluate a priori of the reactivity of the chemical properties from their intrinsic electrical properties. A hard system has a large energy gap while a soft system has a small one. The soft clusters are more reactive than the hard ones because they can easily give electrons to an acceptor.

Oxygen Adsorption on Bimetallic Au_nCu_m (n+m≤5) Clusters

The most stable structures of Au_nCu_mO₂ complexes are displayed in Table 4. It appears that O₂ prefers to bind with Cu in the bimetallic Au_nCu_m clusters. If these structures are compared with the structures of the bare Au_nCu_m clusters, it can be seen that the interaction of the oxygen atom with each cluster only moderately modifies the cluster

geometry. Full geometry optimization has been accomplished for Au_nCu_mO₂ complexes, yielding the adsorption energy, the adsorption height (h), the O-O bond length, and the vibrational frequency. The height h is defined as the shortest Cu-O distance for the Pauling coordination, and it is the vertical distance from the O-O axis to the substrate for the other two coordination modes. The O₂ binding energy is defined by the follow equation:

$$E_b = \left[\frac{-E(\text{Au}_n\text{Cu}_m\text{O}_2) + nE(\text{Au})}{+mE(\text{Cu}) + 2E(\text{O})} \right] / (n + m + 2) \quad (6)$$

The more positive the E_b is, the stronger the bond is. The most stable structures of monometallic and bimetallic Au_nCu_mO₂ occur with the oxygen on-top, binding to the clusters. In these structures, O₂ prefers to bond with the Cu atom.

The adsorption energy is calculated according to the follow equation:

$$E_{\text{ads}} = -E(\text{Au}_n\text{Cu}_m\text{O}_2) + E(\text{O}_2) + E(\text{Au}_n\text{Cu}_m) \quad (7)$$

Where E(Au_nCu_mO₂) is the total energy of the substrate/adsorbate system, E(Au_nCu_m) is the energy of the bare bimetallic cluster, and E(O₂) is the energy of the oxygen molecule.

Our calculations suggested the oxygen on-top as the most stable coordination in the Au₂-O₂, AuCu-O₂, Cu₂-O₂, Au₃O₂, Au₂Cu-O₂, Au₄-O₂, Au₃Cu-O₂, Au₂Cu₂-O₂, AuCu₃-O₂, Cu₄-O₂, and Au₅-O₂ clusters. The bond length of a free oxygen molecule in the gas phase is 1.208 Å [28], and the O-O vibrational frequency is 1580 cm⁻¹[29]. In these complexes, the O-O bond stretches 0.08-0.26Å with respect to the gas phase. The calculated adsorption energies for these structures are in the range of 0.59-2.68eV. The O-O stretching frequencies are in the range of $\nu = 1293.01$ -761.27 cm⁻¹, which indicate a weakening of the O-O bond strength. These features would naturally suggest a net electron flow from the Au or Cu atoms to the oxygen molecules caused the bond weakening of the adsorbed oxygen molecules.

Regarding the complexes with oxygen on bridge site (AuCu₂O₂, Au₄CuO₂, Au₃Cu₂O₂, Au₂Cu₃O₂, AuCu₄O₂, and Cu₅O₂), the O-O bond length (~1.38Å) is 0.18 Å stretched with respect to the gas phase, which falls close to the NEXAFS range of 1.37-0.05Å for the superoxo species. The average adsorption height 'h' is 1.95Å. Taking into consideration the energy of the pure clusters as the reference, the average calculated adsorption energy is 3.08eV.

Table 4: Optimized structure, symmetry, spin multiplicity, dipole moment, average bond length, total energy, vibrational frequency, and IR intensity of Au_nCu_m clusters.

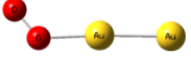
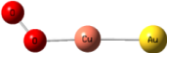
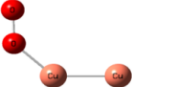
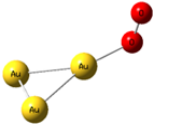
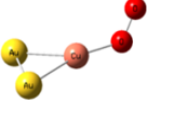
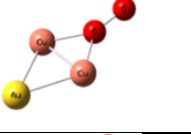

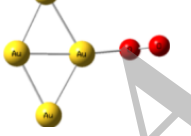
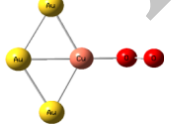
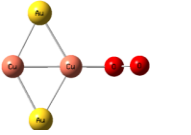
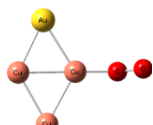
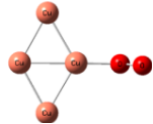
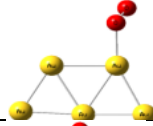
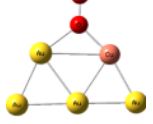
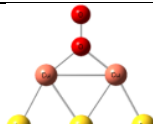
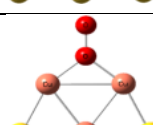
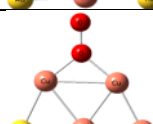
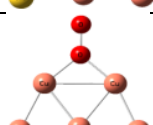
	Symmetry	Spin multiplicity	Dipole moment (Debye)	Average bond length (Å)	Total energy (Hartree)	Vibrational frequency (Cm ⁻¹) (O-O stretching)	IR intensity (Km/mol) (O-O stretching)
	(C _s)	1	0.16	Au-Au 2.53 Au-O 2.16 O-O 1.28	-421.2	1293.0	311.45
	(C _s)	1	0.73	Au-Cu 2.37 Cu-O 1.90 O-O 1.30	-481.9	1280.8	285.72
	(C _s)	1	4.38	Cu-Cu 2.29 Cu-O 1.88 O-O 1.32	-542.6	1203.0	461.29
	(C ₁)	2	2.68	Au-Au 2.72 Au-O 2.12 O-O 1.35	-556.75	1056.35	1648.14
	(C ₁)	2	2.77	Au-Au 2.72 Au-Cu 2.54 Cu-O 1.90 O-O 1.32	-617.47	1153.78	1674.52
	(C _s)	2	2.73	Au-Cu 2.54 Cu-Cu 2.60 Cu-O 1.98 O-O 1.38	-678.17	1079.32	142.55
	(C _{2v})	2	7.55	Cu-Cu 2.37 Cu-O 2.06 O-O 1.40	-738.83	1058.53	147.93
	(C ₁)	1	3.36	Au-Au 2.75 Au-O 2.08 O-O 1.32	-692.22	1185.95	635.10
	(C _s)	1	2.85	Au-Au 2.70 Au-Cu 2.64 O-O 1.31	-752.94	1209.2	568.41
	(C _s)	1	3.80	Au-Cu 2.54 Cu-Cu 2.50 Cu-O 1.89 O-O 1.31	-813.64	1216.62	556.97

Table 4: (Continued) Optimized structure, symmetry, spin multiplicity, dipole moment, average bond length, total energy, vibrational frequency, and IR intensity of Au_nCu_m clusters.

	(C ₁)	1	5.01	Au-Cu 2.53	-874.33	761.62	556.97
				Cu-Cu 2.55			
				Cu-O 1.95			
				O-O 1.46			
	(C ₁)	1	6.10	Cu-Cu 2.42	-934.98	1141.6	572.72
				Cu-O 1.87			
				O-O 1.34			
	(C ₁)	2	3.54	Au-Au 2.76	-827.76	1119.27	1265.07
				Au-O 2.19			
				O-O 1.32			
	(C _s)	2	3.62	Au-Au 2.72	-888.49	1088.23	8.43
				Au-Cu 2.79			
				Cu-O 1.95			
				Au-O 2.20			
	(C _{2v})	2	2.75	O-O 1.37	-949.21	1093.4	12.90
				Au-Au 2.69			
				Au-Cu 2.60			
				Cu-Cu 3.01			
				Cu-O 1.94			
	(C _{2v})	2	3.10	O-O 1.39	-1009.90	1095.58	13.30
				Au-Cu 2.50			
				Cu-Cu 2.73			
				Cu-O 1.93			
	(C _s)	2	4.60	O-O 1.39	-1070.56	1090.87	11.19
				Cu-Cu 2.56			
				Au-Cu 2.51			
	(C _{2v})	2	5.25	Cu-O 1.94	-1131.22	1094.04	10.85
				O-O 1.39			

The average calculated O-O stretching frequency for these structures is 1089.4cm^{-1} . The Cu_3 cluster binds with O_2 (two oxygen atoms bind on top site) with $d_{O-O} = 1.40\text{\AA}$ and $\nu_{O-O} = 1058.53\text{cm}^{-1}$. These features classically suggest the superoxo configuration for the adsorbed O_2 . The dipole moment in a molecule is principally used to study the intermolecular interactions because the higher the dipole moment, the stronger the intermolecular interactions will be. For these $Au_nCu_mO_2$ complexes, Cu_3O_2 has the highest dipole moment (7.55D). The clusters with more Cu atoms have more amounts of the dipole moment which is consistent with the higher electron transfer from

Cu atoms to the oxygen atoms. In the monometallic Au_nO_2 clusters, the dipole moment increases with an increase in the number of Au atoms.

The E_b and the E_{ads} are shown in Fig. 2. The E_{ads} for the systems, which do not display dissociation of the oxygen molecule, has values ranging from 0.6 to 3.6 eV; these values were the maximum for the $Au_2Cu_3O_2$ system. As shown in Fig. 2, the binding and the adsorption energies generally decrease gradually with the increase in the number of copper atoms in the bimetallic cluster. However, $AuCu_2O_2$, $Au_2Cu_3O_2$, and $Au_3Cu_2O_2$ systems show maximum binding energies and assent with systems that have the high adsorption energy. It

can similarly be observed that the systems with minimum binding energy also have the lowest adsorption energy, e.g., for AuCuO₂, Au₂O₂, and Au₃CuO₂ systems.

Fig. 3 also displays other fine behavior when the magnitude of the O-O distance and the O-O stretching frequency are compared. It indicates that an increase in the O-O distance produces a decrease in the O-O frequency. The O-O frequency of the adsorbed O₂ molecule has values ranging from 761.6 to 1293.0 cm⁻¹, i.e., from 51% to 18% lower than the O-O frequency for the O₂ in the gas phase (1580 cm⁻¹). These behaviors clarify that the charge transfer from the bimetallic clusters to the empty orbitals of oxygen weakens the O-O bond,

causing an elongation of up to 17% in comparison to its gas-phase length, as noted in the previous section, and reduces its stretching frequency.

The HOMO-LUMO gap, shown in Fig. 4, was studied because it is a measure of the relative chemical reaction to the molecular hardness [30]. The gap is compared with the adsorption energy for the Au_nCu_mO₂ systems with respect to the number of gold and copper atoms in the bimetallic cluster.

Generally, it can be observed that systems presenting high adsorption energy, also present a large HLG, i.e., the adsorption systems tend to increase the molecular hardness and this produces a high reactivity.

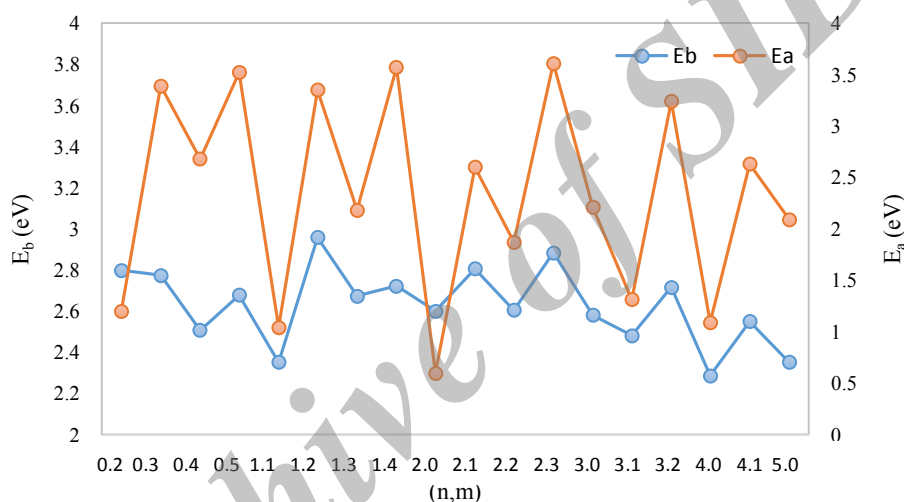


Fig. 2: Binding energy and adsorption energy for Au_nCu_mO₂ complexes

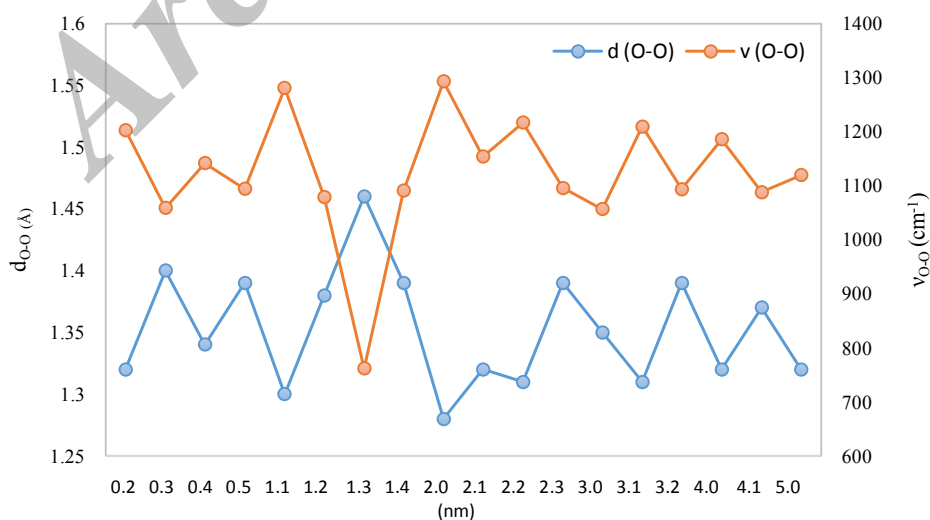


Fig. 3: O-O bond distance and stretching frequency for the adsorbed oxygen in Au_nCu_mO₂ complexes

Fig. 5 also shows the difference in gaps between the $Au_nCu_mO_2$ and Au_nCu_m systems and adsorption energy. It is showing that the greater the difference in the gap, the greater the adsorption energy. The largest difference in the gap is observed for $AuCu_4O_2$ and $Au_2Cu_3O_2$ systems.

This indicates that with the increase in the number of copper atoms in the bimetallic clusters, the system present high adsorption energy, i.e., the high reactivity toward the oxygen molecule. In the $AuCuO_2$ bimetallic cluster, the difference between gaps is presented as negative values,

i.e., the gap of $Au_nCu_mO_2$ is smaller than the gap of Au_nCu_m , showing a low reactivity to the adsorption of molecular oxygen.

To gain an overall view of the electronic structures of $Au_nCu_mO_2$ complexes, the total DOS for these systems are shown in Fig. 6. The oxygen adsorption on the clusters associated with significant electron transfer from metal atoms to molecular oxygen empty orbitals; also notable is the nearness of the band of the occupied states to the Fermi level of the metal and to the band of the lowest unoccupied states.

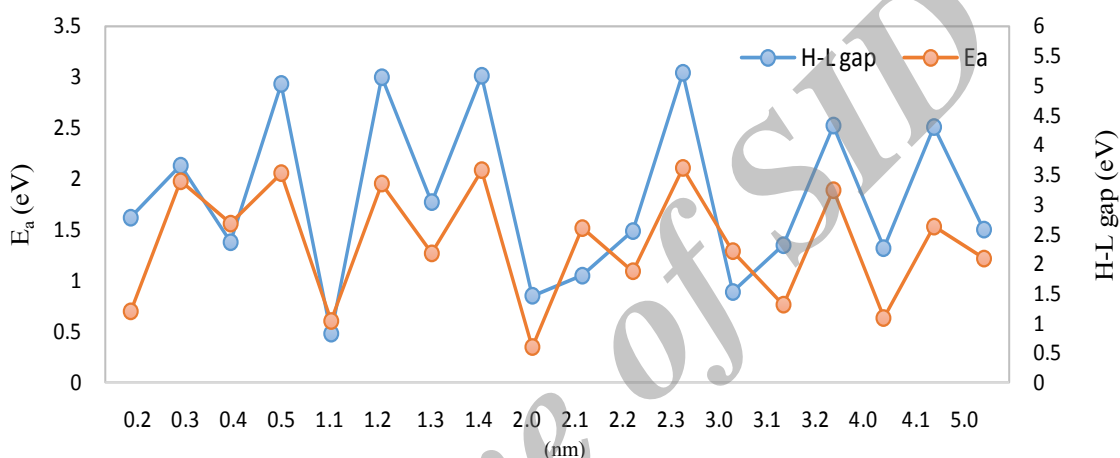


Fig. 4: Adsorption energy and gap between frontier orbitals, LUMO–HOMO (H-L gap), for $Au_nCu_mO_2$ complexes.

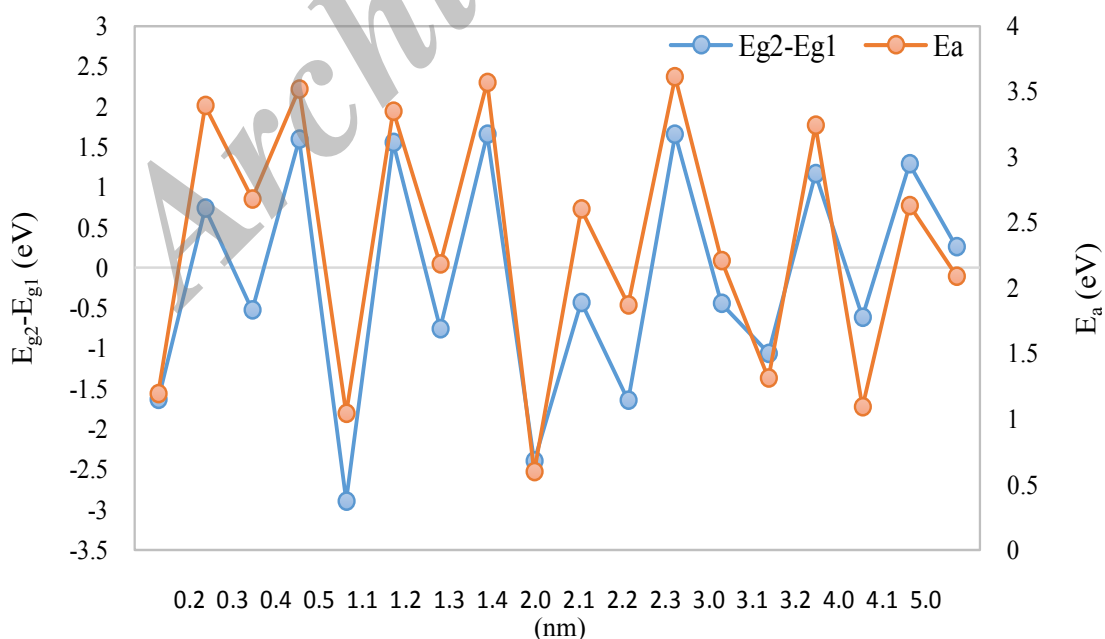


Fig. 5. Adsorption energy and difference of gaps [$E_{g2}-E_{g1} = E_g(Au_nCu_mO_2) - E_g(Au_nCu_m)$]; $E_g = E_{LUMO} - E_{HOMO}$.

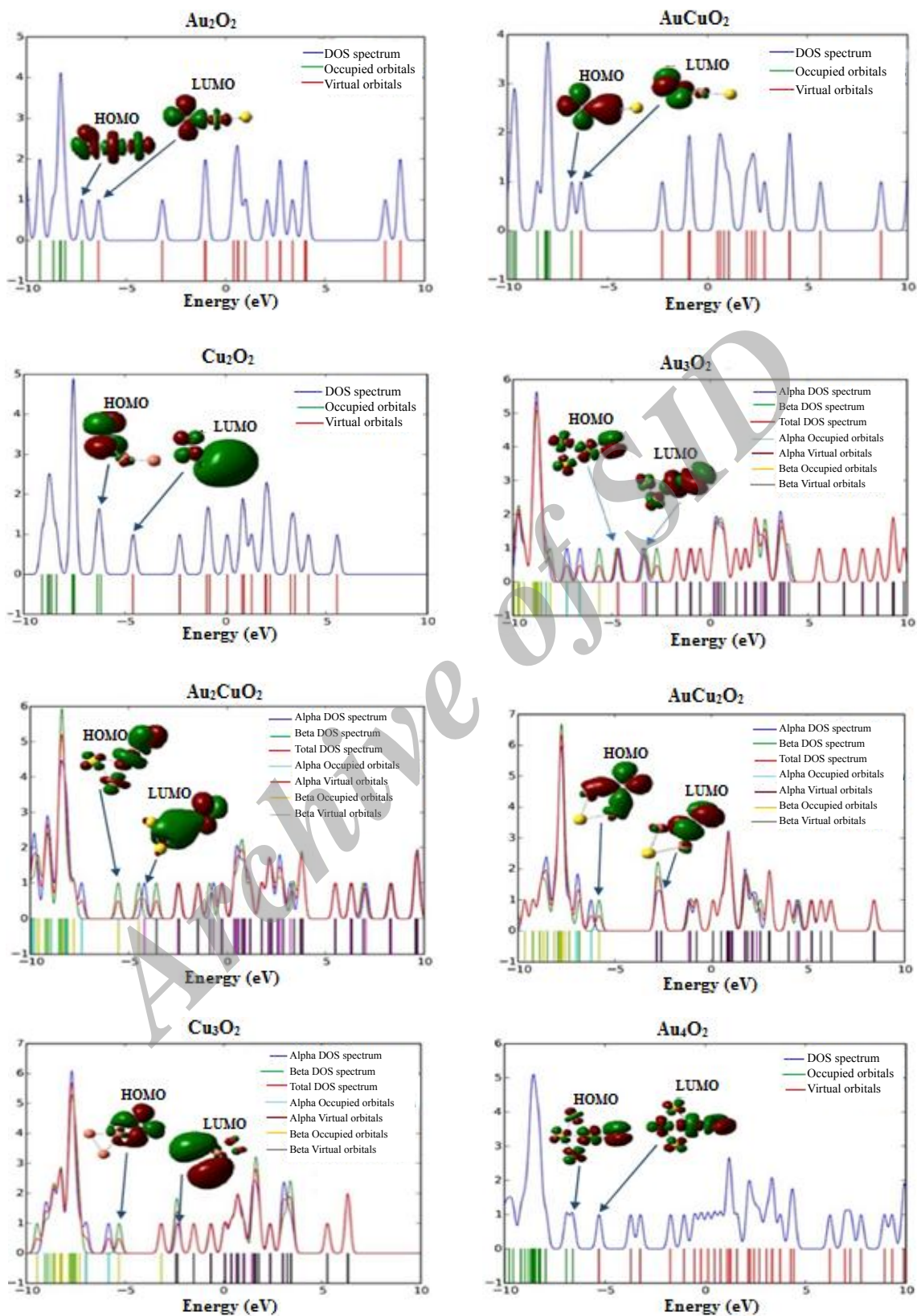


Fig. 6: Density of states, spatial orientation of HOMO and LUMO of $Au_nCu_mO_2$ complexes.

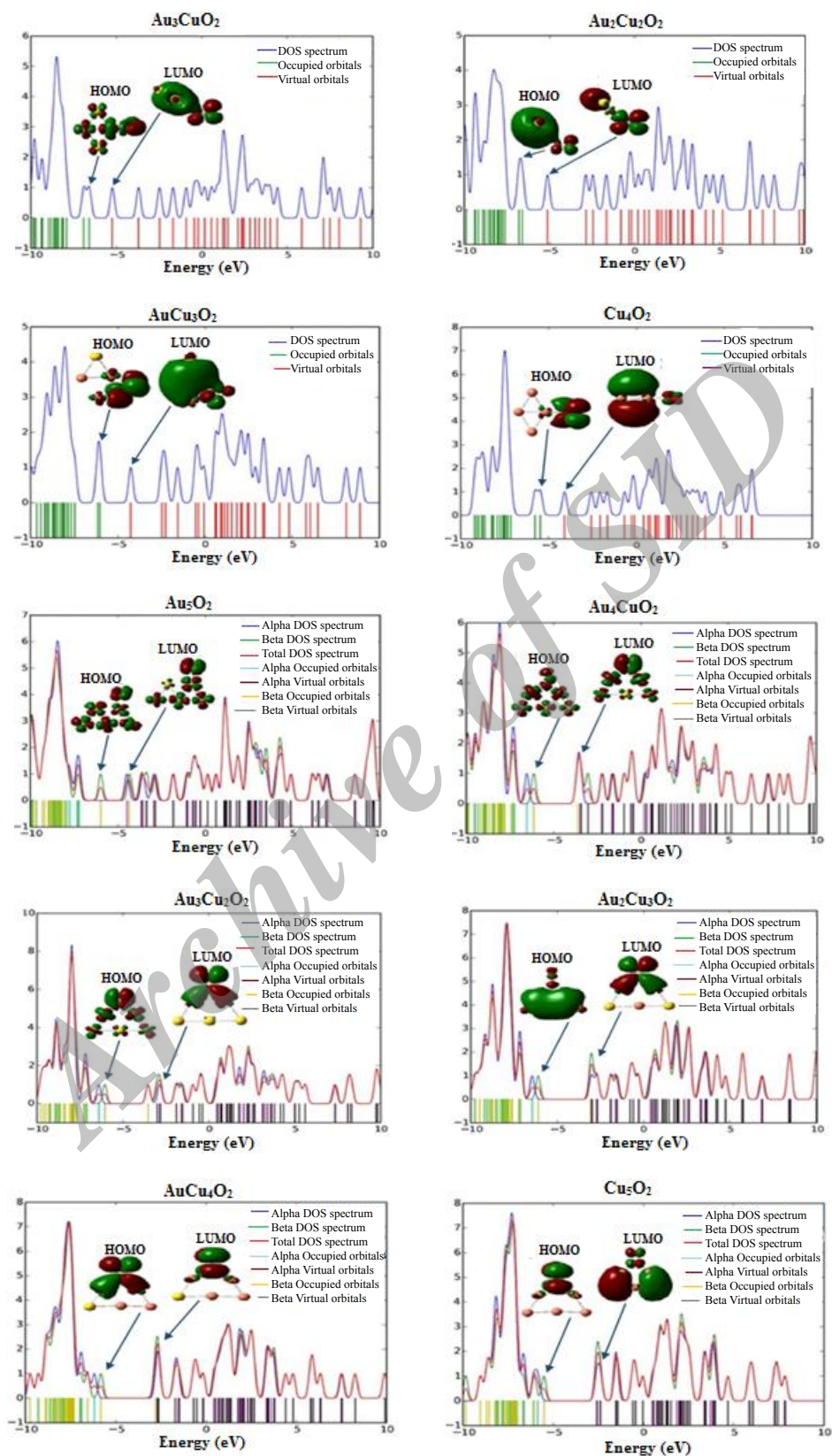


Fig. 6: (Continued) Density of states, spatial orientation of HOMO and LUMO of $Au_nCu_mO_2$ complexes.

CONCLUSIONS

In this study, DFT-GGA calculations were performed to investigate the Au/Cu clusters consisting of 2-5 atoms with various structures and compositions. The binding energy, dipole moment, vibrational frequency, IR intensity as well as the HOMO-LUMO energy gap and the electronic DOS were obtained. The results demonstrated that the planar configuration was the most stable structure among the Au/Cu clusters. Also, eighteen O₂-Au/Cu complexes were investigated. It was found that the reactivity of O₂ on bimetallic Au_nCu_m clusters was higher than that for the monometallic Au_n and Cu_n clusters. Further, the results showed that the O₂ adsorptions to the Cu site were stronger than to the Au site. For bimetallic clusters, the O₂ molecule preferred to adsorb at the Cu site rather than at the Au site. Furthermore, the HOMO-LUMO energy gap changed upon O₂ adsorption. The adsorption process occurred such that a high symmetry was maintained in the adsorption system. The interaction between the clusters and O₂ was energetically favorable when the O₂ was adsorbed at a bridge site. After the adsorption of the O₂ molecule, the enhancement of reactivity of O₂ was obvious, appearing as the shortening of Au-Cu bond length and the lengthening of O-O bond length. The strongest adsorption existed in the AuCu₄ cluster. Although its bulk material is chemically inert, gold in cluster form showed a good reactivity for oxygen adsorption as with the copper clusters.

ACKNOWLEDGMENTS

We thank the Iran Nanotechnology Initiative Council for financial support.

CONFLICT OF INTEREST

The authors declare that there is no conflict of interests regarding the publication of this manuscript.

REFERENCES

- [1] Ekardt W., (1999), *Metal Clusters*, First ed., USA: Wiley-VCH.
- [2] Zhai H. J., Wang L. S., (2005), Chemisorption sites of CO on small gold clusters and transitions from chemisorption to physisorption. *J. Chem. Phys.* 122: 051101-051111.
- [3] Kadossov E., Justin J., Lu M., Rosenmann D., Ocola L. E., Cabrini S., Burghaus U., (2009), Gas-surface interactions with nanocatalysts: Particle size effects in the adsorption dynamics of CO on supported gold clusters. *Chem. Phys. Lett.* 483: 250-256.
- [4] Liu X., Wang A., Wang X., Mou C. Y., Zhang T., (2008), Au-Cu alloy nanoparticles confined in SBA-15 as a highly efficient catalyst for CO oxidation. *Chem. Commun.* 27: 3187-3191.
- [5] Andrews M. P., O'Brien S. C., (1992), Gas-phase "molecular alloys" of bulk immiscible elements: iron-silver (Fe_xAg_y). *J. Phys. Chem.* 96: 8233-8237.
- [6] Lang S. M., Claes P., Cuong N. T., Nguyen M. T., Lievens P., Janssens E., (2011), Copper doping of small gold cluster cations: influence on geometric and electronic structure. *J. Chem. Phys.* 135: 224305-224311.
- [7] Zhao Y. R., Kuang X. Y., Zheng B. B., Li Y. F., Wang S. J., (2011), Equilibrium geometries, stabilities, and electronic properties of the bimetallic M₂-doped Au_n (M = Ag, Cu; n = 1-10) clusters: comparison with pure gold clusters. *J. Phys. Chem. A* 115: 569-575.
- [8] Kuang X., Wang X., Liu G., (2011), Structural, electronic and magnetic properties of small gold clusters with a copper impurity. *Trans. Met. Chem.* 36: 643-649.
- [9] Wang H. Q., Kuang X. Y., Li H. F., (2010), Density functional study of structural and electronic properties of bimetallic copper-gold clusters: comparison with pure and doped gold clusters. *Phys. Chem. Chem. Phys.* 12: 5156-5161.
- [10] Zorriastein S., Joshi K., Kanhere D. G., (2008), Electronic and structural investigations of gold clusters doped with copper: Au_{n-1}Cu₁ (n=13-19). *J. Chem. Phys.* 128: 184314-7.
- [11] Parr R. G., Yang W., (1989), *Density-Functional Theory of Atoms and Molecules*, New York: Oxford University Press.
- [12] Lee C., Yang W., Parr R. G., (1988), Development of the Colle-Salvetti correlation-energy formula into a functional of the electron density. *Phys. Rev. B* 37: 785-788.
- [13] Wadt W. R., Hay P. J., (1985), Ab initio effective core potentials for molecular calculations. Potentials for the transition metal atoms Sc to Hg. *J. Chem. Phys.* 82: 270-275.
- [14] Zhao Y., Li Z., Yang J., (2009), A density functional study on cationic Au_nCu_m⁺ clusters and their monocarbonyls. *Phys. Chem. Chem. Phys.* 11: 2329-2335.
- [15] Bishea G. A., Pinegar J. C., Morse M. D., (1991), the ground state and excited d-hole states of CuAu. *J. Chem. Phys.* 95: 5630-5636.
- [16] Frisch M. J., Trucks G. W., Schlegel H. B., Scuseria G. E., Robb M. A., Cheeseman J. R., Montgomery J. A., Vreven T., Kudin K. N., Burant J. C., Millam J. M., Iyengar S. S., Tomasi J., Barone V., Mennucci B., Cossi M., Scalmani G., Rega N., Petersson G. A., Nakatsuji H., Hada M., Ehara M., Toyota K., Fukuda R., Hasegawa J., Ishida M., Nakajima T., Honda Y., Kitao O., Nakai H., Klene M., Li X., Knox J. E., Hratchian H. P., Cross J. B., Bakken V., Adamo C., Jaramillo J., Gomperts R., Stratmann R. E., Yazyev O., Austin A. J., Cammi R., Pomelli C., Ochterski J., Ayala P. Y., Morokuma K., Voth G. A., Salvador P., Dannenberg J. J., Zakrzewski V. G., Dapprich S., Daniels A. D., Strain M. C., Farkas O., Malick D. K., Rabuck A. D., Raghavachari K., Foresman J. B., Ortiz J. V., Cui Q., Baboul A. G., Clifford S., Cioslowski J., Martin R. L., Fox D. J., Keith T., Al-Laham M. A., Peng C. Y., Nanayakkara A., Challacombe M., Gill P. M. W., Johnson B. G., Chen W., Wong M. W., Gonzalez C., Pople J. A., (2004), *Gaussian 03, Revision E.01*, Gaussian, Inc., Wallingford: CT.
- [17] Zhao S., Lu W. W., Ren Y. L., Wang J. J., Yin W. P., (2012), Density functional study of NO_x binding on small Au_nCu_m (n + m ≤ 5) clusters. *Comp. Theor. Chem.* 993: 90-95.
- [18] Wang H. Q., Kuang X. Y., Li H. F., (2010), Density functional study of structural and electronic properties of bimetallic copper-gold clusters: comparison with pure and doped gold clusters. *Phys. Chem. Chem. Phys.* 12: 5156-5159.
- [19] Huber K. P., Herzberg G., (1979), *Molecular Spectra and Molecular Structure: Constants of Diatomic Molecules*, New York: Van Nostrand.
- [20] Jackslath C., Rabin I., Schulze W., (1992), Electronic Structures and Related Properties. *Electron Impact*

- Ionization Potentials of Gold and Silver Clusters Me_n ; $n \leq 22$. *Phys. Chem.* 96: 1200-1206.
- [21] Rohlfling E. A., Valentini J. J., (1986), UV laser excited fluorescence spectroscopy of the jet-cooled copper dimer. *J. Chem. Phys.* 84: 6560-6567.
- [22] Kuang X., Wang X., Liu G., (2011), Structural, electronic and magnetic properties of small gold clusters with a copper impurity. *Trans. Met. Chem.* 36: 643-648.
- [23] Zhao Y. R., Kuang X. Y., Zheng B. B., Li Y. F., Wang S. J., (2011), Equilibrium geometries, stabilities, and electronic properties of the bimetallic M_2 -doped Au_n ($M = Ag, Cu$; $n = 1-10$) clusters: comparison with pure gold clusters. *J. Phys. Chem. A.* 115: 569-575.
- [24] Zhao Y., Li Z., Yang J., (2009), A density functional study on cationic Au_nCu_m clusters and their monocarbonyls. *Phys. Chem. Chem. Phys.* 11: 2329-2336.
- [25] Wang H. Q., Kuang X. Y., Li H. F., (2010), Density functional study of structural and electronic properties of bimetallic copper-gold clusters: comparison with pure and doped gold clusters. *Phys. Chem. Chem. Phys.* 12: 5156-5161.
- [26] Zhan C. G., Nichols J. A., Dixon, D. A., (2003), Ionization Potential, Electron Affinity, Electronegativity, Hardness, and Electron Excitation Energy: Molecular Properties from Density Functional Theory Orbital Energies. *J. Phys. Chem. A.* 107: 4184-4189.
- [27] Pearson R. G., (1997), *Chemical Hardness: Applications from Molecules to Solids*, Weinheim: Wiley-VCH.
- [28] Greenwood N. N., Earnshaw A., (1984), *Chemistry of Elements*, Oxford: Pergamon Press.
- [29] Huber K. P., Herzberg G., (1979), *Molecular Spectra and Molecular Structure: Constants of Diatomic Molecules*, New York: Van Nostrand Reinhold.
- [30] Parr R. G., Pearson R. G., (1983), Absolute hardness: companion parameter to absolute electronegativity. *J. Am. Chem. Soc.* 105: 7512-7516.